Electronic Supporting Information: Dynamics of nanoparticle tracers in supercooled nanoparticle matrices

Peter Edimeh, Ali H. Slim, and Jacinta C. Conrad*

Determination of the matrix volume fraction ϕ

The volume fraction ϕ of polystyrene (PS) particles within a suspension was determined by tracking the mass of the sample before and after samples were concentrated via centrifugation. First, the masses of the empty centrifuge membrane M_{m} and filter tube M_{ft} were determined. Using a pipette, 400 μL of the PS suspension with $\phi_{PS} = 10\%$ (mass M_{t}) was transferred into the centrifuge apparatus and the total mass of the centrifuge assembly (membrane, filter, and suspension) M_{asm} was measured. The initial mass of the PS suspension M_{s} was calculated by subtracting the mass of the assembled empty components from the mass of the assembly containing the suspension $M_{\mathrm{s}} = M_{\mathrm{asm}} - (M_{\mathrm{m}} + M_{\mathrm{ft}}$. We estimated that the mass of PS particles $M_{\mathrm{PS}} = 0.1 M_{\mathrm{s}}$ (based on the weight fraction) and then calculated the volume of PS particles $V_{\mathrm{PS}}/\rho_{\mathrm{PS}}$, where $\rho_{\mathrm{PS}} = 1.055 \times 10^{12}$ g $\mu\mathrm{m}^{-3}$. Similarly, the mass of water $M_{\mathrm{w}} = M_{\mathrm{s}} - M_{\mathrm{PS}}$ and the volume of water $V_{\mathrm{w}} = M_{\mathrm{w}}/\rho_{\mathrm{w}}$, where $\rho_{\mathrm{w}} = 0.997 \times 10^{12}$ g $\mu\mathrm{m}^{-3}$. The total suspension volume was $V_{\mathrm{t}} = V_{\mathrm{PS}} + V_{\mathrm{w}}$, leading to the initial volume fraction $\phi_i = V_{\mathrm{PS}}/V_{\mathrm{t}}$.

Suspensions were centrifuged at 8000 rpm for a given duration depending on desired ϕ. We measured the mass of the membrane + residue, $M_{\mathrm{m+r}}$ and the mass of the filter tube containing the filtrate $M_{\mathrm{ft+f}}$ and subsequently determined the residue mass $M_{\mathrm{r}} = M_{\mathrm{m+r}} - M_{\mathrm{m}}$ and filtrate mass $M_{\mathrm{f}} = M_{\mathrm{ft+f}} - M_{\mathrm{ft}}$. The residue contained PS particles along with a small amount of water of mass $M_{\mathrm{r,w}} = M_{\mathrm{r}} - M_{\mathrm{PS}}$. The volume of water in the residue was then $V_{\mathrm{r,w}} = M_{\mathrm{r,w}}/\rho_{\mathrm{w}}$. We assumed that the the volume of PS in the residue did not change, i.e. $V_{\mathrm{r,PS}} = M_{\mathrm{PS}}/\rho_{\mathrm{PS}}$. The total volume of the residue $V_{\mathrm{r}} = V_{\mathrm{r,w}} + V_{\mathrm{r,PS}}$. Finally, we determined $\phi = V_{\mathrm{PS}}/V_{\mathrm{r}}$. This process was designed to achieve an absolute The error on the determination of ϕ within 3%, consistent with the typical The error in determining colloidal ϕ[1]. We note, however, that ϕ is increased through the duration of centrifugation, and so the relative volume fractions are consistent.

Tracking resolution ϵ

δ	ϕ	G:W	Δx (μm)	ϵ (μm)	N (pixel $\times$ pixel)	N(μm $\times$ μm)
0.71	≤ 0.45	5:6	0.228	0.155	256 $\times$ 256	58.4 $\times$ 58.4
0.71	> 0.45	5:6	0.152	0.105	256 $\times$ 256	38.9 $\times$ 38.9
0.45	≥ 0.45	6:5	0.114	0.059	256 $\times$ 256	29.2 $\times$ 29.2
0.36	≤ 0.46	6:5	0.114	0.255	256 $\times$ 256	29.2 $\times$ 29.2
0.36	> 0.46	6:5	0.091	0.214	256 $\times$ 256	23.3 $\times$ 23.3
0.34	≤ 0.45	6:5	0.091	0.231	256 $\times$ 256	23.3 $\times$ 23.3
0.34	> 0.45	6:5	0.076	0.175	256 $\times$ 256	19.5 $\times$ 19.5

Table S1: Values of the tracking resolution ϵ for the given tracer-matrix size ratio (δ), glycerol: water mixing ratio (G:W), and volume fraction (ϕ) values; Δx is the pixel size used in each series of experiments and N is the 2D-image size in (pixel $\times$ pixel) and (μm $\times$ μm).

Supplementary tracking figures

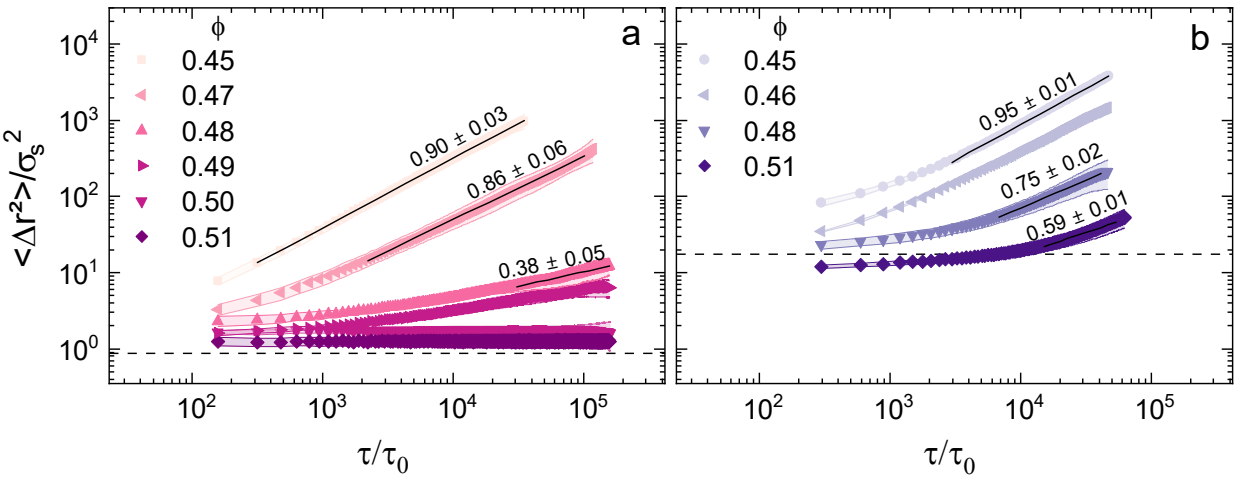

Figure S1: Ensemble averaged mean-squared displacement (MSD) $\langle \Delta r^2 \rangle$ normalized by tracer diameter σ_s^2 as a function of lag time τ normalized by Brownian diffusion time τ_0 for various ϕ at size ratios δ of (a) 0.45 and (b) 0.36. Solid black lines indicate the scaling exponent α, where MSD $\propto \tau^\alpha$. The MSD is diffusive when $\alpha = 1$ and subdiffusive when $\alpha < 1$. The dashed lines represent the normalized tracking resolution ϵ. The The error bars indicate one standard deviation over at least four replicates per state point.

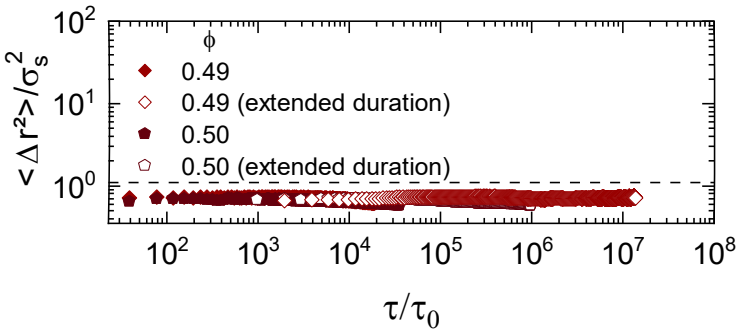

Figure S2: Normalized MSD $\langle r^2 \rangle / \sigma_s^2$ as a function of normalized lag time τ/τ_0, where τ_0 is the Brownian diffusion time for the large tracer, $\delta = 0.71$ at $\phi = 0.49$ and 0.50.

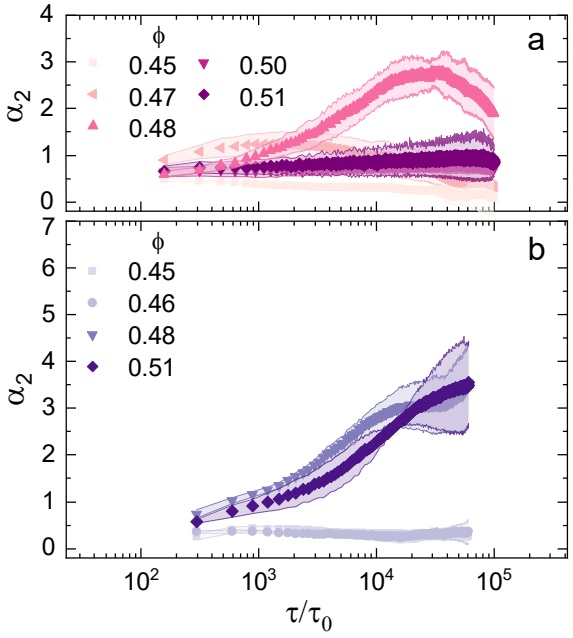

Figure S3: Non-Gaussian parameter α_2 as a function of normalized lag time τ/τ_0, where τ_0 is the Brownian diffusion time for each tracer, at various ϕ for size ratio δ values of (a) 0.45 and (b) 0.36. The error bars indicate one standard deviation over at least four replicates per state point.

Differential dynamic microscopy

δ	ϕ	Δx (μm)	$q_{\min}$ (μm^{-1})
0.71	≤ 0.45	0.228	0.108
0.71	> 0.45	0.152	0.161
0.45	≥ 0.45	0.114	0.215
0.36	≤ 0.46	0.114	0.215
0.36	> 0.46	0.091	0.270
0.34	≤ 0.45	0.091	0.270
0.34	> 0.45	0.076	0.323

Table S2: Pixel size Δx and theoretical minimum $q_{\min}$ for the various samples.

$\phi = 0.45$								$\phi = 0.46$			
$\delta = 0.71$		$\delta = 0.45$		$\delta = 0.36$		$\delta = 0.34$		$\delta = 0.36$		$\delta = 0.34$	
$q\sigma_s$	s	$q\sigma_s$	s	$q\sigma_s$	s	$q\sigma_s$	s	$q\sigma_s$	s	$q\sigma_s$	s
0.07	0.82	0.07	0.92	0.07	0.90	0.06	0.80	0.07	0.91	0.06	0.91
0.11	0.91	0.11	0.92	0.08	0.85	0.09	0.80	0.08	1.0	0.09	1.0
0.15	0.91	0.14	0.94	0.09	0.82	0.12	0.85	0.09	1.0	0.12	0.99
0.24	0.91	0.16	0.93	0.11	0.82	0.14	0.66	0.11	0.98	0.14	0.97
0.39	0.90	0.22	0.94	0.15	0.88	0.21	0.67	0.22	0.81	0.23	0.86
0.56	0.88	0.27	0.94	0.18	0.88	0.23	0.78	0.26	0.75	0.27	0.78
0.73	0.83	0.33	0.93	0.22	0.75						
0.90	0.78	0.38	0.93	0.26	0.89						
1.04	0.71	0.43	0.92								
1.24	0.59	0.50	0.88								
$\phi = 0.47$						$\phi = 0.48$		$\phi = 0.49$		$\phi = 0.50$	
$\delta = 0.71$		$\delta = 0.45$		$\delta = 0.34$		$\delta = 0.36$		$\delta = 0.34$		$\delta = 0.34$	
$q\sigma_s$	s	$q\sigma_s$	s	$q\sigma_s$	s	$q\sigma_s$	s	$q\sigma_s$	s	$q\sigma_s$	s
0.07	0.80	0.07	0.81	0.06	0.83	0.07	0.74	0.06	0.66	0.06	0.63
0.10	0.71	0.11	0.78	0.09	0.70	0.08	0.72	0.09	0.61	0.10	0.52
0.16	0.63	0.16	0.74	0.12	0.70	0.10	0.62	0.14	0.63	0.16	0.40
0.23	0.62	0.22	0.74	0.14	0.63	0.15	0.51	0.20	0.64		
0.36	0.60	0.38	0.61	0.23	0.65	0.20	0.46	0.23	0.59		

Table S3: Stretching exponent s from fits of the ISFs to a stretched exponential function $f(q,\tau) = \exp\{-(\Gamma(q)\tau)^s\}$ at specified normalized wavevectors $q\sigma_s$ for various samples.

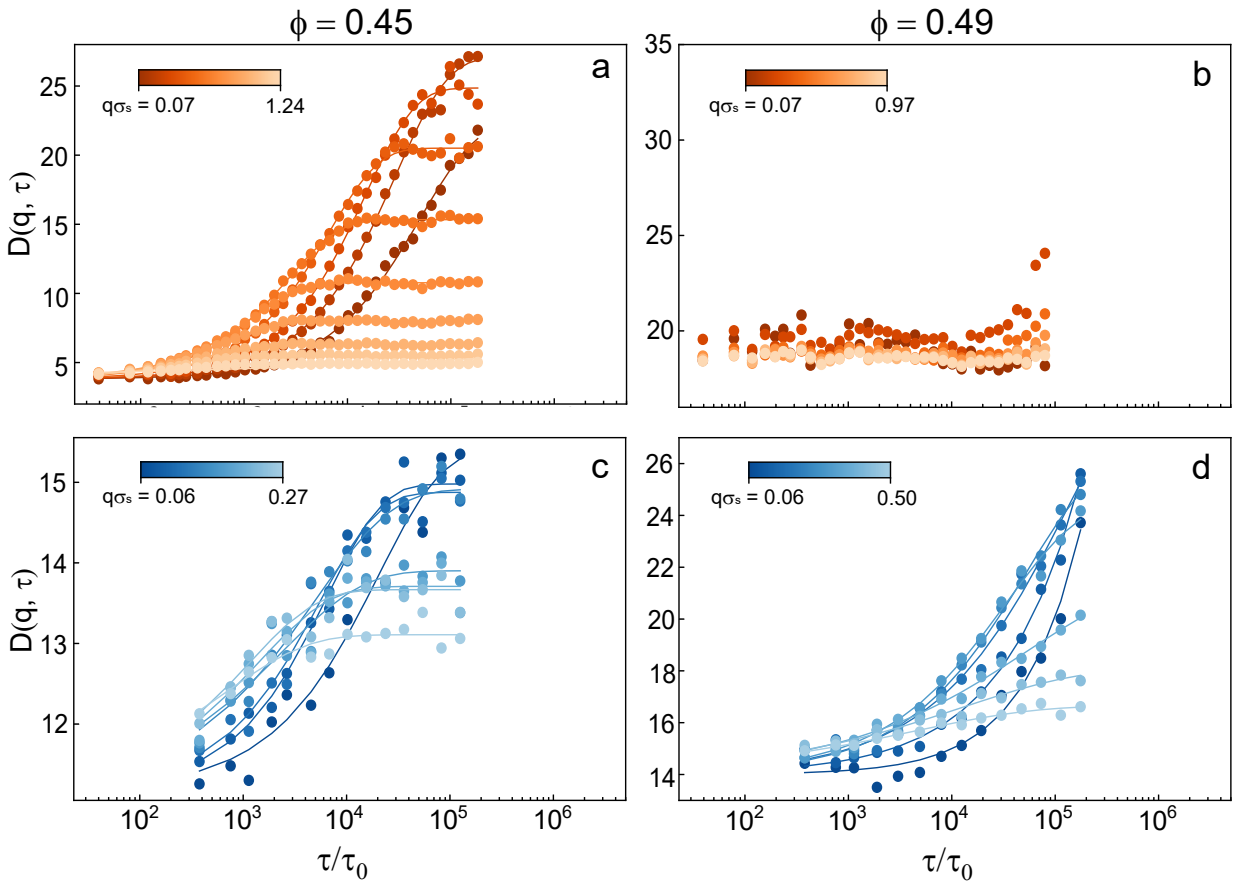

Figure S4: DDM structure function $D(q, \Delta\tau)$ for (a) (δ, ϕ) = (0.71, 0.45), (b) (δ, ϕ) = (0.71, 0.49), (c) (δ, ϕ) = (0.34, 0.45), and (d) (δ, ϕ) = (0.34, 0.49).

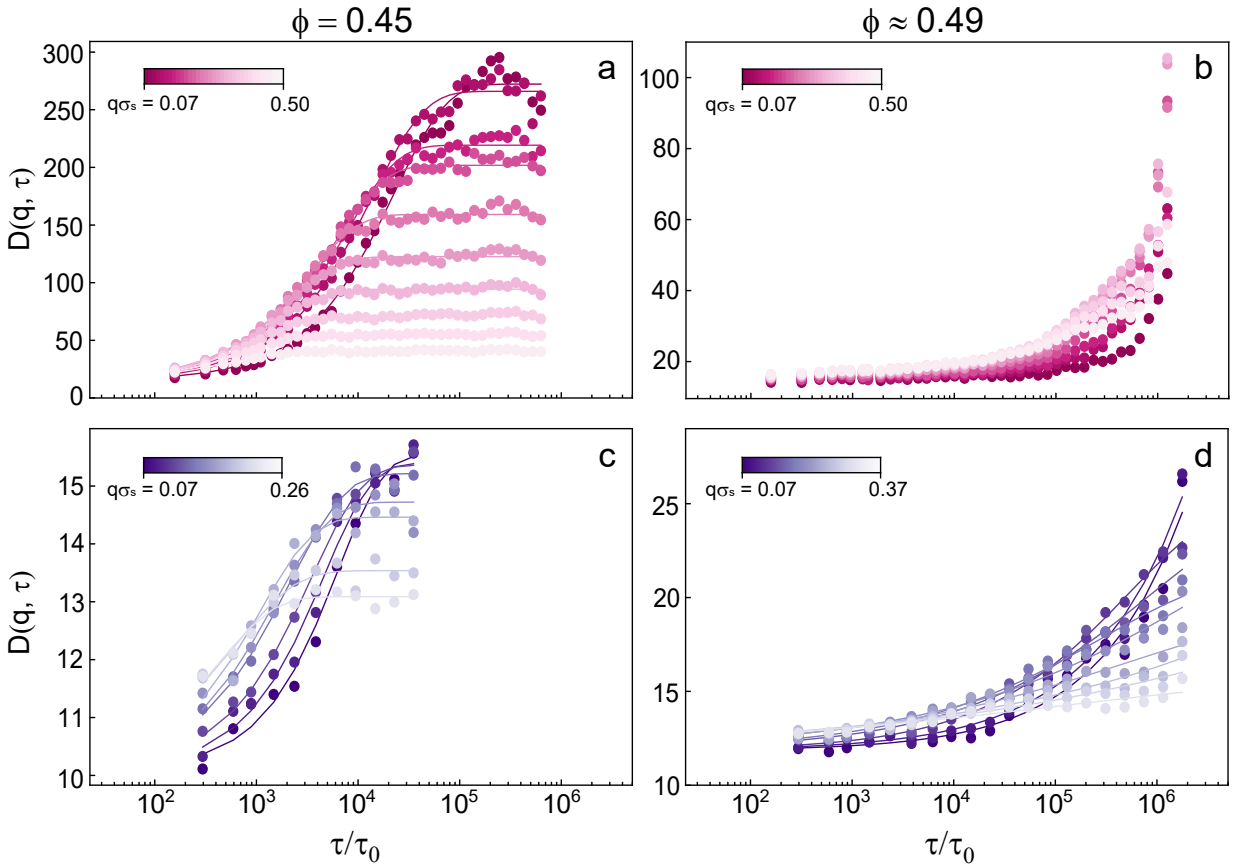

Figure S5: DDM structure function $D(q, \Delta\tau)$ for (a) $(\delta, \phi) = (0.45, 0.45)$, (b) $(\delta, \phi) = (0.45, 0.49)$, (c) $(\delta, \phi) = (0.36, 0.45)$, and (d) $(\delta, \phi) = (0.36, 0.48)$.

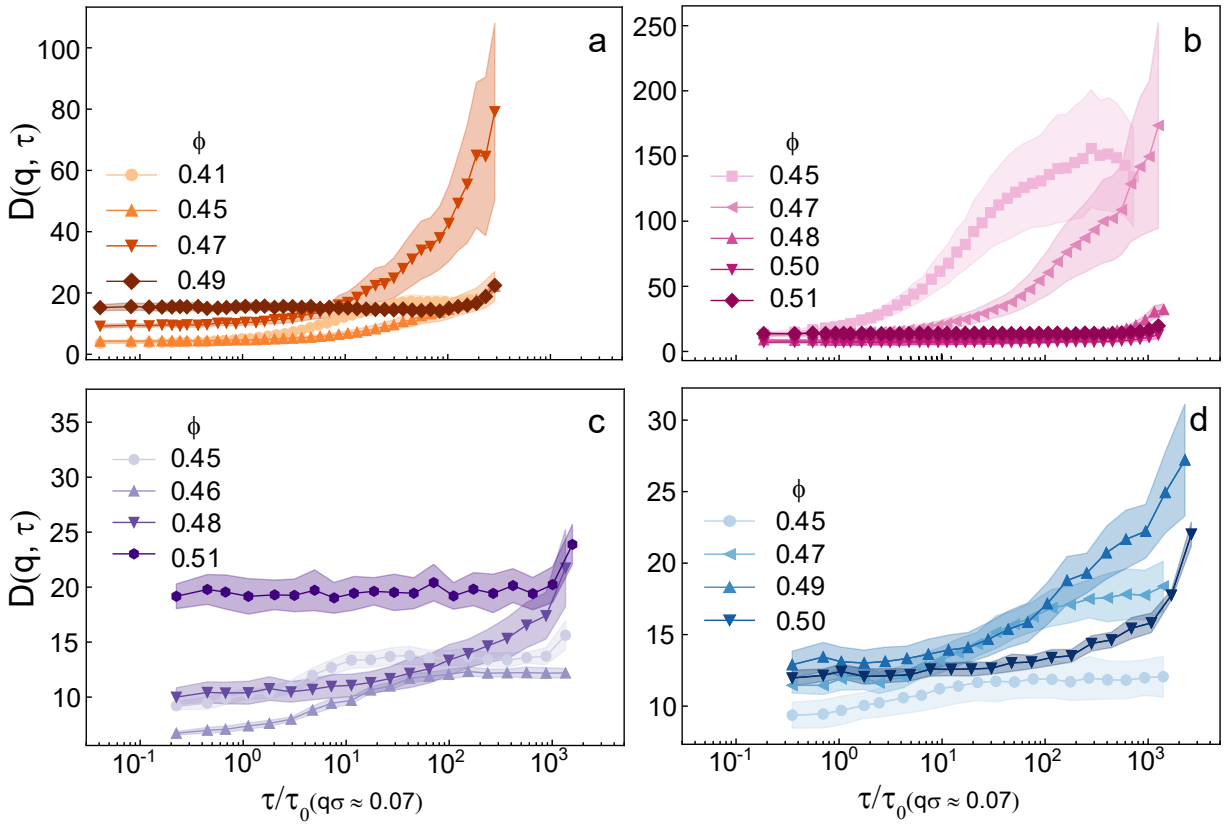

Figure S6: DDM structure function $D(q, \Delta\tau)$ as a function of τ/τ_0 and ϕ at $q\sigma_s \sim 0.07$ for (a) $\delta = 0.71$, (b) $\delta = 0.45$, (c) $\delta = 0.36$, and (d) $\delta = 0.34$. The error bars correspond to standard deviation of the averaged measurements.

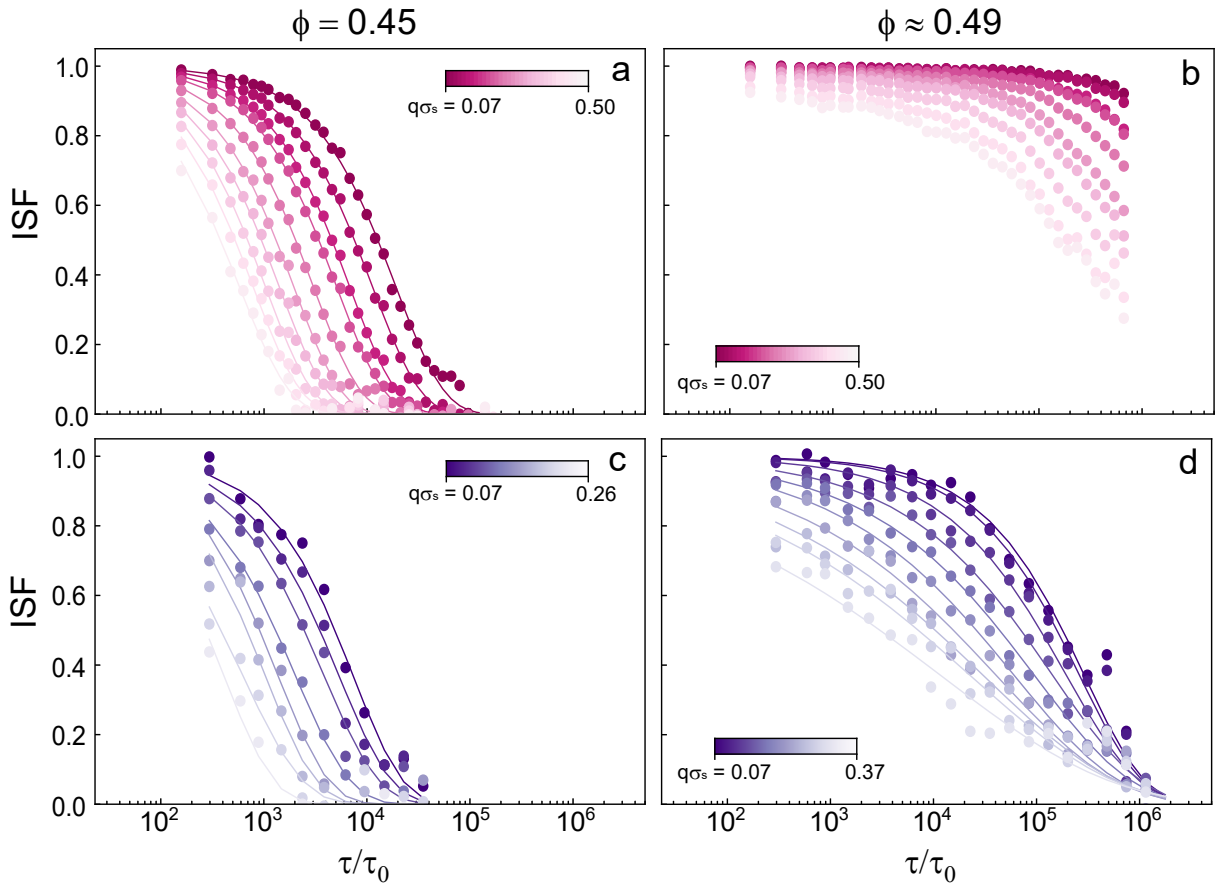

Figure S7: Collective intermediate scattering function $f(q,\tau)$ as a function of normalized lag τ/τ_0 for exhibits single exponential decay for $(\delta,\ \phi)$ = (a) (0.45, 0.45), (b) (0.45, 0.49), (c) (0.36, 0.45), and (d) (0.36, 0.48). The lines in (a), (c), and (d) indicate fits of the data to a single exponential decay.

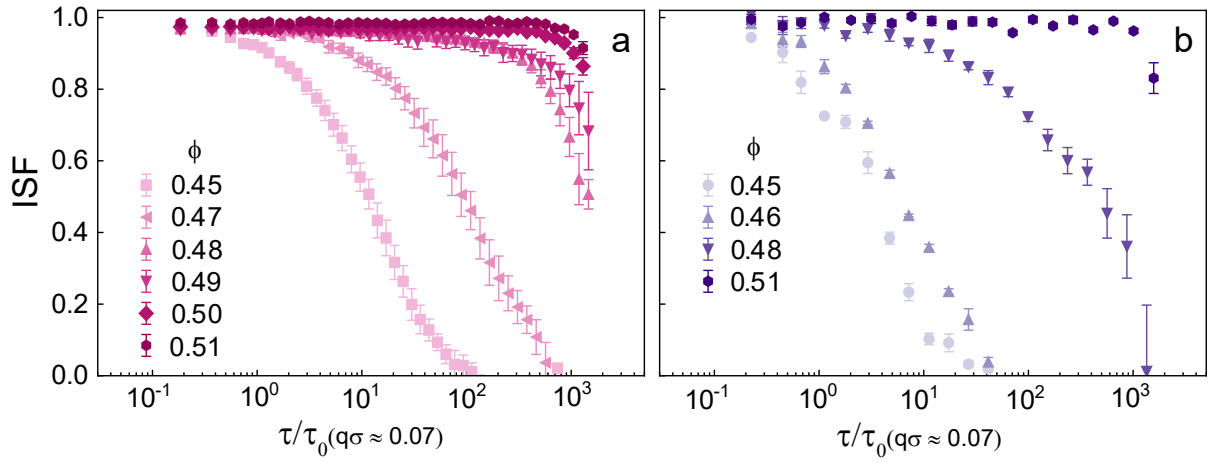

Figure S8: Intermediate scattering function $f(q,\tau)$ as a function of τ/τ_0 and ϕ at $q\sigma_s \sim 0.07$ for δ of (a) 0.45 and (b) 0.36. The error bars correspond to standard deviation of the averaged measurements.

Comparison of self-intermediate scattering functions from DDM and SPT

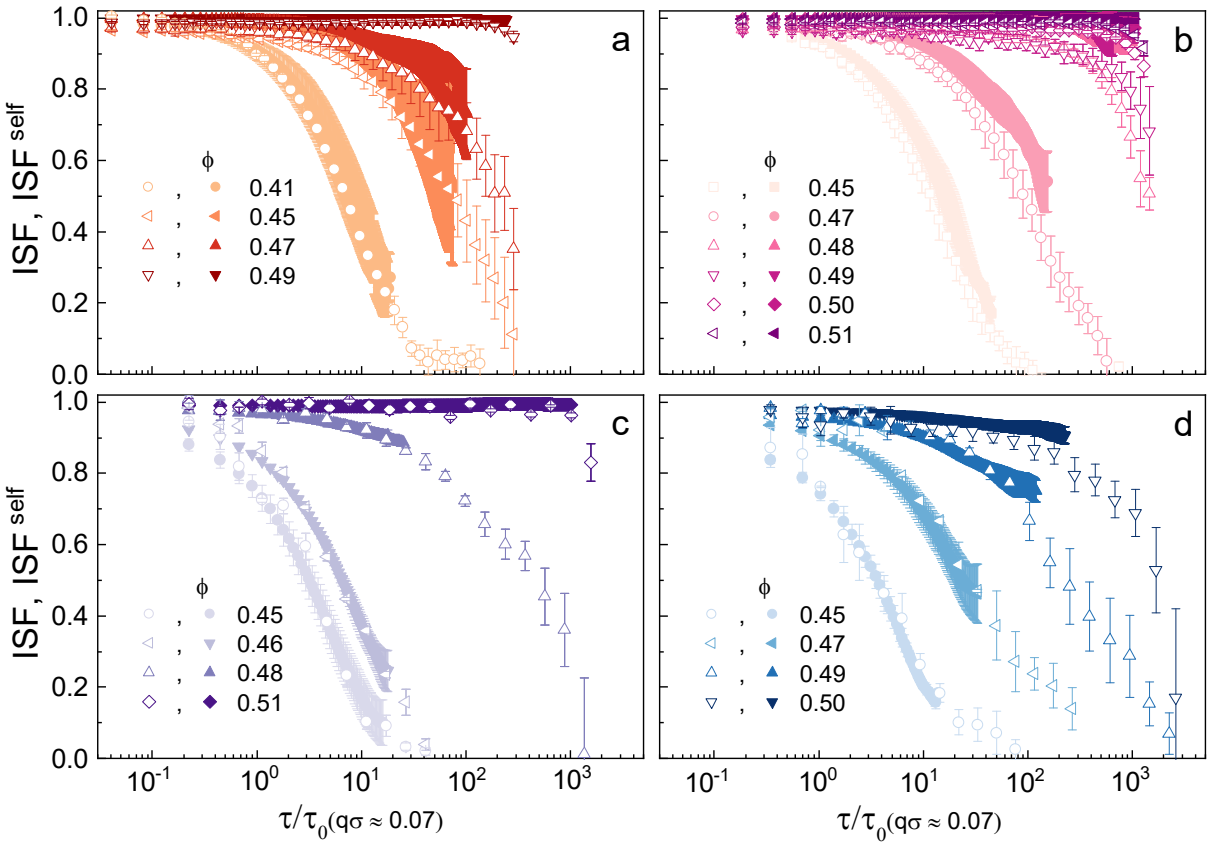

Figure S9: $f(q,\tau)$ and $f^{\text{self}}(q,\tau)$ as a function of τ/τ_0 and ϕ at $q\sigma_s \sim 0.07$ for (a) $\delta = 0.71$, (b) $\delta = 0.45$, (c) $\delta = 0.36$, and (d) $\delta = 0.34$. Open symbols represent $f(q,\tau)$, and closed symbols represent $f^{\text{self}}(q,\tau)$. The error bars correspond to standard deviation of the averaged measurements. $f^{\text{self}}(q,\tau)$ was calculated from tracer trajectories obtained from SPT using $f^{\text{self}}(q,\tau) = \frac{1}{N}\sum_{m=1}^{N}\left\langle e^{-j\mathbf{q}\cdot[\mathbf{r}_m(t_0+\tau)-\mathbf{r}_m(t_0)]}\right\rangle_{|\mathbf{q}|=q,t_0}$.[2]

Effective diameter mapping

To account for the electrostatic interactions between particles, we calculate the repulsive potential $\beta U(D) = \pi\sigma_{\text{nom}}\epsilon\zeta^2 \exp(-\kappa D)$ as a function of distance D between particle surfaces in the low surface charge limit, where $\beta = (k_B T)^{-1}$ is the inverse thermal energy, σ_{nom} is the nominal particle diameter, ϵ is the solvent permittivity, and κ^{-1} is the Debye screening length. The suspensions were prepared in deionized water, but no care was taken to ensure that suspensions were near-salt-free. Thus, we calculate the repulsive potential for $\kappa^{-1} = 1$ nm and 10 nm, which approximately span the values reported for DI water in a non-salt-free environment. The effective hard sphere diameter σ_t is then obtained using the Barker-Henderson formalism[3] $\sigma_{\text{eff}} = \sigma_{\text{nom}} + \int [1 - \exp\{-\beta U(D)\}]\, dD$. The nominal sizes σ_{nom}, zeta potentials ζ, and calculated effective sizes σ_{eff} are shown in Table S4 and S5.

σ_{nom} (nm)	ζ (mV)	σ_{eff} (nm)	δ_{nom}	δ_{eff}
47	-21 ± 6	50.0 ± 0.5	0.34	0.34
51	-27 ± 3	54.6 ± 0.2	0.36	0.38
63	-37 ± 3	67.5 ± 0.2	0.45	0.46
100	-40 ± 4	105.1 ± 0.2	0.71	0.72
120	-39 ± 4	125.2 ± 0.2	-	-
140	-37 ± 6	145.3 ± 0.3	-	-

Table S4: Nominal particle diameter σ_{nom}, zeta potential ζ, effective diameter σ_{eff}, nominal size ratio δ_{nom} and effective size ratio δ_{eff} for Debye length $\kappa^{-1} = 1$ nm

σ_{nom} (nm)	ζ (mV)	σ_{eff} (nm)	δ_{nom}	δ_{eff}
47	-21 ± 6	77 ± 5	0.34	0.40
51	-27 ± 3	87 ± 2	0.36	0.45
63	-37 ± 3	107 ± 2	0.45	0.56
100	-40 ± 4	151 ± 2	0.71	0.78
120	-39 ± 4	172 ± 2	-	-
140	-37 ± 6	192 ± 3	-	-

Table S5: Nominal particle diameter σ_{nom}, zeta potential ζ, effective diameter σ_{eff}, nominal size ratio δ_{nom} and effective size ratio δ_{eff} for Debye length $\kappa^{-1} = 10$ nm

Determination of logarithmic relaxations

Logarithmic relaxations were identified by fitting $f(q,\tau)$ data for each wavevector to the logarithmic function: $f(q,\tau) = a \cdot \ln(\tau) + b$, where a and b are fitting parameters. We classified a given $f(q,\tau)$ curve as classified as exhibiting a logarithmic relaxation if the fit could be successfully performed over at least two decades in time. Figure S10 shows examples of the logarithmic fits applied to selected $f(q,\tau)$ curves.

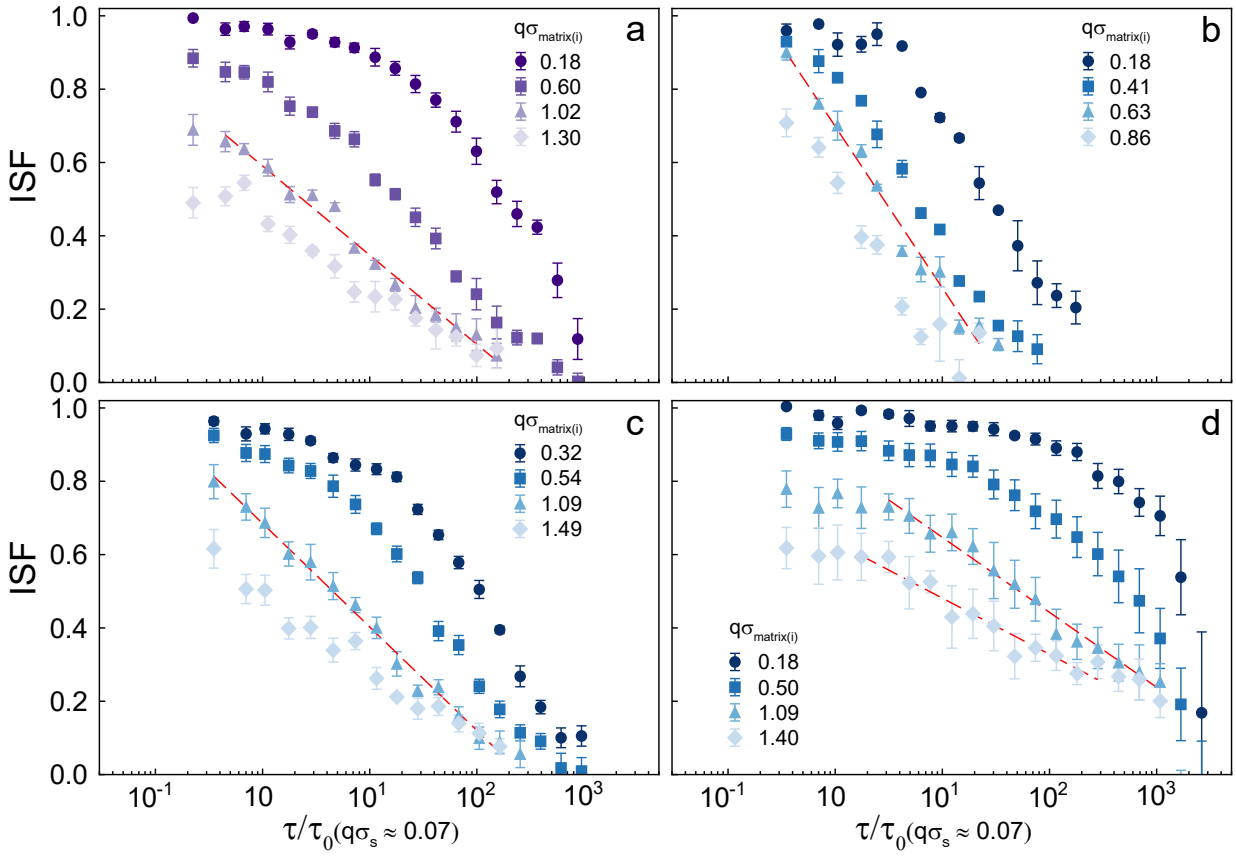

Figure S10: Intermediate scattering function $f(q,\tau)$ as a function of τ/τ_0 and ϕ at $q\sigma_s \sim 0.07$ for exhibiting anomalous logarithmic decays of $f(q,\tau)$ for at least two decades in time for (a) $(\delta,\phi) = (0.36,\ 0.48)$, (b) $(\delta,\phi) = (0.34,\ 0.47)$, (c) $(\delta,\phi) = (0.34,\ 0.49)$ and (d) $(\delta,\phi) = (0.34,\ 0.50)$. The error bars correspond to standard deviation of the averaged measurements.

δ	ϕ	$q^*\sigma_{\text{matrix(i)}}$	L^* $(\sigma_{\text{matrix(i)}})$	Number of time decades
0.34	0.47	0.63	9.93	2
	0.49	1.09	5.76	2.5
	0.50	1.09	5.76	2.5
	0.50	1.40	4.49	2
0.36	0.48	1.02	6.16	2.5

Table S6: Samples exhibiting anomalous logarithmic decays of in $f(q,\tau)$ of at least two decades in time: wave vector $q^*\sigma_{\text{matrix(i)}}$, corresponding length scale in units of $\sigma_{\text{matrix(i)}}$ and time span of decay

References

[1] W. C. K. Poon, E. R. Weeks and C. P. Royall, *Soft Matter*, 2012, **8**, 21–30.

[2] F. Giavazzi, V. Trappe and R. Cerbino, *Journal of Physics: Condensed Matter*, 2020, **33**, 024002.

[3] J. A. Barker and D. Henderson, *The Journal of Chemical Physics*, 1967, **47**, 2856–2861.